CHIN. PHYS. LETT. Vol. 38, No. 8 (2021) 088801

Coulomb Thermoelectric Drag in Four-Terminal Mesoscopic Quantum Transport

Mengmeng Xi(席萌萌)[1], Rongqian Wang(王荣倩)[2], Jincheng Lu(陆金成)[2,3*], and Jian-Hua Jiang(蒋建华)[2*]

[1]*Hefei National Laboratory for Physical Sciences at Microscale, University of Science and Technology of China, Hefei 230026, China*

[2]*School of Physical Science and Technology & Collaborative Innovation Center of Suzhou Nano Science and Technology, Soochow University, Suzhou 215006, China*

[3]*Center for Phononics and Thermal Energy Science, China-EU Joint Lab on Nanophononics, Shanghai Key Laboratory of Special Artificial Microstructure Materials and Technology, School of Physics Science and Engineering, Tongji University, Shanghai 200092, China*

(Received 10 April 2021; accepted 7 June 2021; published online 2 August 2021)

We show that the Coulomb interaction between two circuits separated by an insulating layer leads to unconventional thermoelectric effects, such as the cooling by thermal current effect, the transverse thermoelectric effect and Maxwell's demon effect. The first refers to cooling in one circuit induced by the thermal current in the other circuit. The middle represents electric power generation in one circuit by the temperature gradient in the other circuit. The physical picture of Coulomb drag between the two circuits is first demonstrated for the case with one quantum dot in each circuit and it is then elaborated for the case with two quantum dots in each circuit. In the latter case, the heat exchange between the two circuits can vanish. Finally, we also show that the Maxwell's demon effect can be realized in the four-terminal quantum dot thermoelectric system, in which the quantum system absorbs the heat from the high-temperature heat bath and releases the same heat to the low-temperature heat bath without any energy exchange with the two heat baths. Our study reveals the role of Coulomb interaction in non-local four-terminal thermoelectric transport.

DOI: 10.1088/0256-307X/38/8/088801

Thermoelectric transport is a useful tool to study the fundamental properties of quasiparticles in mesoscopic systems.[1] Abundant information of quasiparticle dynamics and fluctuations, phase coherence and statistics can be revealed in thermoelectric transport.[2–4] Most existing research has focused on elastic thermoelectric transport, such as ballistic transport and resonant tunneling in mesoscopic systems.[5–13] There has only recently been a surge of interest in studying thermoelectric transport involving inelastic processes where electron energy is not conserved during the transport. It was found that inelastic thermoelectric devices can provide higher efficiency and larger output power than conventional elastic thermoelectric devices made of the same material.[14–31] Furthermore, several unconventional effects, such as the cooling by heating effect[32–34] and the linear-response thermal transistor effect,[35–39] have been discovered in inelastic thermoelectric devices. It was also proven that these effects cannot take place in an elastic thermoelectric device.

Several types of inelastic thermoelectric devices have been studied, including electron-phonon[40–43] or electron-electron interaction.[41,44–52] In general, electron-phonon interaction is more important at high temperatures, whereas electron-electron interactions are important at very low temperatures. In this work, we will show the inelastic thermoelectric transport at the low-temperature regime and discuss the key role of the electron-electron interaction in it.

It has been shown that in a three-terminal device with one quantum dot (QD), electronic noises (essentially heat energy) from the third terminal can induce electrical power generation for the source and drain terminals.[14,53] The underlying mechanism is the inelastic Coulomb scattering, which induces a directional transport when the left-right inversion symmetry is broken as in other quantum ratchets. In these studies, heat in the third electronic terminal is harvested to produce electrical energy across the source and the drain. Recently, Whitney *et al.* found that in a four-terminal QD thermoelectric device, electrical energy across the source and the drain can be produced by harvesting heat from two additional capacitively coupled terminals.[54] Remarkably, the produced electrical energy is finite when the total heat

Supported by the Science and Technological Fund of Anhui Province for Outstanding Youth (Grant No. 1508085J02), the National Natural Science Foundation of China (Grant Nos. 61475004, 11675116, and 12074281), the Chinese Academy of Sciences (Grant No. XDA04030213), the Jiangsu Distinguished Professor Funding and a Project Funded by the Priority Academic Program Development of Jiangsu Higher Education Institutions (PAPD), and the China Postdoctoral Science Foundation (Grant No. 2020M681376).

*Corresponding authors. Email: jincheng.lu1993@gmail.com; jianhuajiang@suda.edu.cn

© 2021 Chinese Physical Society and IOP Publishing Ltd

injected into the QD system vanishes.

In this work, we show that cooling of the source in a four-terminal mesoscopic system can be achieved by passing a perpendicular heat current between the two additional terminals, even if these two terminals do not exchange charge with the source or the drain. The cooling by heat current effect is driven by the Coulomb drag between electrons in the two circuits even though they are separated by a charge insulation layer. This effect may happen in a number of four-terminal mesoscopic thermoelectric systems when the Coulomb interaction between two circuits is strong. Here, we focus on illustration of the effect via correlated transport through Coulomb coupled QDs with particular spatial symmetries. These symmetries are realized by engineering the energy dependent coupling between the QDs and the four terminals. With a simple two-QD setup, the cooling by heat current effect can be realized. In a setup with two pairs of double QDs, the cooling by heat current effect can be realized with the total heat exchanged between the two circuits vanishes. This limit is consistent with the thermodynamic analysis that the cooling of the source is driven by the heat flow in the other circuit from the hot terminal to the cold terminal, instead of the total heat flux exchanged between the two circuits.

Four-Terminal Quantum-Dots Thermoelectric Systems. We first consider a four-terminal double QDs thermoelectric system, which is illustrated in Fig. 1. The system can be regarded as two independent circuits without Coulomb interaction. The source, the drain and the upper quantum dot form a circuit, while the other two electrodes and the lower quantum dot form another circuit. The two circuits are separated by an insulating layer. Thermoelectrics in the two circuits are correlated once the interaction between electrons in the two QDs are considered. In general, Coulomb interaction between the two QDs can cause drag effect and inelastic thermoelectric transport in the two circuits, which leads to unconventional thermoelectric phenomena. To demonstrate the underlying physics, we will consider the Coulomb interaction of the following form,[14]

$$H_{\text{Coulomb}} = E_{\text{C}} n_1 n_2, \tag{1}$$

where n_1 and n_2 are the numbers of electrons in the two QDs, respectively. E_{C} is the strength of Coulomb interaction. We will show in this work that such a simple interaction leads to novel thermoelectric phenomena in four-terminal systems.

Beside the source and the drain, there are other two electrodes (electronic reservoirs). In our setup, their electrochemical potentials are set to the equilibrium value so that they serve as "heat baths"; i.e., charge motions between them do not produce or consume any electrical energy. We thus consider only the heat current flowing out of the H reservoir, J_{H}, and the heat current flowing into the C reservoir, J_{C} (we suppose $T_{\text{H}} > T_{\text{C}}$, where T_{H} and T_{C} are the temperature of the heat bath H and C, respectively.). In contrast, the source and the drain can have potentials differing from the equilibrium value, leading to charge motion under (self-consistent) electrical fields. We hence consider both the charge current between the source and the drain, J_{e}, and the heat current flowing out of (into) the source (drain) terminal, J_{S} (J_{D}).

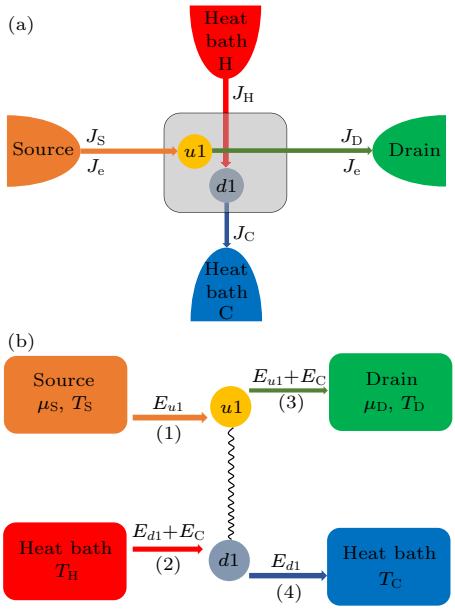

Fig. 1. (a) Schematic of the four-terminal QDs thermoelectric system. Beside the source and the drain, there are two other electrodes, H and C. Only the heat currents flowing out/into these electrodes are considered because their electrochemical potentials are set to the equilibrium value. In experiments, these two electrodes (termed as "heat baths") and the QD $d1$ are fabricated in a lower layer. In the upper layer, there are the source, the drain, and the QD $u1$. The lower and upper layers are separated by an insulating layer (depicted as the gray shadow). Electrons in the two QDs interact with each other via Coulomb (repulsive) interaction. (b) Illustration of correlated electron transport through the QDs $u1$ and $d1$. An electron tunnels between the source and the QD $u1$ only at energy E_{u1} (i.e., when there is no electron in the QD $d1$). The electron tunnels between the drain and the QD $u1$ can only take place at energy $E_{u1} + E_{\text{C}}$ (i.e., with an electron in the QD $d1$). For the QD $d1$, electron tunnels between the heat bath H and the QD only at energy $E_{d1} + E_{\text{C}}$ (i.e., when there is an electron in the QD $u1$). The electron tunnels between the QD $d1$ and the heat bath C only at energy E_{d1}. The interaction between electron, depicted as the wavy lines, is the crucial element for the correlated inelastic transport through the QDs $u1$ and $d1$. For the electron motion indicated by the arrows, an energy E_{C} is pumped into the source and drain subsystem from the H and C subsystem.

Although there are four heat currents, energy conservation imposes the following restriction,[55]

$$J_{\text{S}} + \frac{\mu_{\text{S}}}{e} J_{\text{e}} + J_{\text{H}} = J_{\text{C}} + J_{\text{D}} + \frac{\mu_{\text{D}}}{e} J_{\text{e}}, \tag{2}$$

where $\mu_{\rm S}$ and $\mu_{\rm D}$ are the electrochemical potentials of the source and the drain, respectively. It is useful to consider the following combinations

$$J_{\rm in} = J_{\rm H} - J_{\rm C}, \quad J_q = \frac{1}{2}(J_{\rm H} + J_{\rm C}). \tag{3}$$

Here $J_{\rm in}$ can be understood as the total heat injected into the QDs system from the two heat baths H and C. J_q is regarded as the heat flow (exchange) between the reservoirs H and C. We will choose the independent heat currents as three of the four heat currents; e.g., $J_{\rm S}$, $J_{\rm in}$ and J_q. The affinities corresponding to the three heat currents and the electrical current can be found by analyzing the total entropy production,[55–57]

$$\partial_t S_{\rm tot} = \sum_i J_i A_i, \tag{4a}$$

$$A_{\rm e} = \frac{\mu_{\rm S} - \mu_{\rm D}}{eT_{\rm D}}, \quad A_{\rm S} \equiv \frac{1}{T_{\rm D}} - \frac{1}{T_{\rm S}}, \tag{4b}$$

$$A_{\rm in} \equiv \frac{1}{T_{\rm D}} - \frac{1}{2T_{\rm H}} - \frac{1}{2T_{\rm C}}, \quad A_q \equiv \frac{1}{T_{\rm C}} - \frac{1}{T_{\rm H}}. \tag{4c}$$

To demonstrate the underlying physics, in the following we will consider the simple situation where there is only a single energy level that allows tunneling from each electrode to the connected QD.

We now present the microscopic theory for thermoelectric transport in the QDs system. Explicitly, we shall construct the expressions for the electrical and heat currents as functions of the electrochemical potentials, $\mu_{\rm S}$ and $\mu_{\rm D}$, as well as the temperatures, $T_{\rm S}$, $T_{\rm D}$, $T_{\rm H}$ and $T_{\rm C}$. As shown in Fig. 1(b), we consider particular configurations where QDs $u1$ and $d1$ are capacitively coupled, whereas there is no other coupling between QD $u1$ and other QDs. We also assume that the intradot Coulomb repulsion is so strong that double occupancy is forbidden. In these configurations, the energies for electrons in the QDs are given by

$$E_{u1,n_{d1}} = E_{u1} + n_{d1}E_{\rm C}, \tag{5a}$$

$$E_{d1,n_{u1}} = E_{d1} + n_{u1}E_{\rm C}, \tag{5b}$$

$$n_{u1}, n_{d1} = 0, 1. \tag{5c}$$

Here, E_{u1} and E_{d1} are the electron energies for QDs $u1$ and $d1$ if there is no interaction between QDs; n_{u1} and n_{d1} denote the numbers of electrons in the $u1$ and $d1$ QDs, respectively.

To realize the cooling by heat current effect through the Coulomb interaction, we consider the four-terminal four-QD thermoelectric system; as shown in Fig. 2(a). In this particular configuration, QDs $u2$ and $d2$ are capacitively coupled, whereas there is no other coupling between QD $u2$ and other QDs [see Fig. 2(b)].

Similarly, the expressions hold for QDs $u2$ and $d2$ are

$$E_{u2,n_{d2}} = E_{u2} + n_{d2}E_{\rm C}, \tag{6}$$

$$E_{d2,n_{u2}} = E_{d2} + n_{u2}E_{\rm C}, \tag{7}$$

$$n_{u2}, n_{d2} = 0, 1. \tag{8}$$

For simplicity, we have assumed that the charge interaction strength between the QDs $u2$ and $d2$ are the same as that for the QDs $u1$ and $d1$. Transport through QDs system can actually be divided into two parts: the four-terminal transport through the pair of QDs $u1$ and $d1$ and that through the pair of QDs $u2$ and $d2$. These two channels are *independent* of each other.

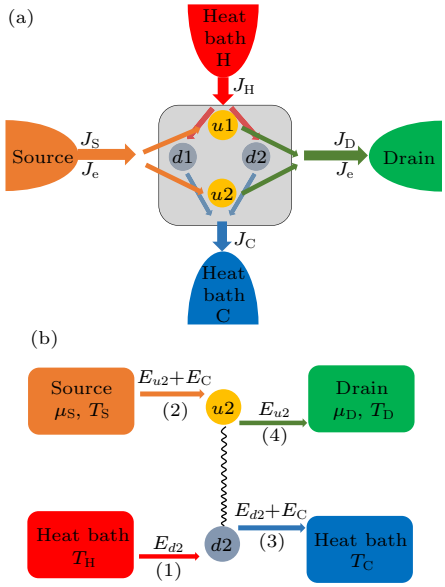

Fig. 2. (a) Schematic of the four-terminal QDs thermoelectric system. Beside the source and the drain, there are two other electrodes. Only the heat currents flowing out/in these electrodes are considered because their electrochemical potentials are set to the equilibrium value. In experiments, these two electrodes (termed as "heat baths") and the two QDs $d1$ and $d2$ can be fabricated in a lower layer. The source and drain electrodes together with the QDs $u1$ and $u2$ can be fabricated in the upper layer. The lower layer and the upper layer are separated by an insulating layer (depicted as the gray shadow). However, electrons in the QDs can interact with each other via the long range Coulomb interaction. (b) Correlated electron tunneling through the QDs $u2$ and $d2$. Similar to electron tunneling through the $u1$ and $d1$ QDs, with different energy configurations for electron tunneling. For electron motion indicated by the arrows in the figure, an energy $E_{\rm C}$ is provided by the source and drain subsystem to the H and C subsystems. The arrows indicate one possible direction of electron motion, which can be reversed, depending on the voltage and temperature biases. The numbers in the brackets indicate the sequences of the correlated tunneling processes.

The electrical and heat currents can be expressed as (see the Supplemental Material)

$$J_{\rm e} = e\sum I_i, \tag{9a}$$

$$J_{\rm S} = E_{u1}I_1 + (E_{u2}+E_{\rm C})I_2, \tag{9b}$$
$$J_{\rm H} = (E_{d1}+E_{\rm C})I_1 + E_{d2}I_2, \tag{9c}$$
$$J_{\rm C} = E_{d1}I_1 + (E_{d2}+E_{\rm C})I_2, \tag{9d}$$
$$J_{\rm in} = E_{\rm C}(I_1 - I_2), \tag{9e}$$
$$J_q = \Big(E_{d1}+\frac{1}{2}E_{\rm C}\Big)I_1 + \Big(E_{d2}+\frac{1}{2}E_{\rm C}\Big)I_2, \tag{9f}$$

where

$$I_1 = \gamma_1^{-1}(k^+_{u1,0}k^+_{d1,1}k^-_{u1,1}k^-_{d1,0} - k^+_{d1,0}k^+_{u1,1}k^-_{d1,1}k^-_{u1,0}),$$
$$I_2 = \gamma_2^{-1}(k^+_{d2,0}k^+_{u2,1}k^-_{d2,1}k^-_{u2,0} - k^+_{u2,0}k^+_{d2,1}k^-_{u2,1}k^-_{d2,0}), \tag{10}$$

and

$$\gamma_1 = \sum_{\alpha=u1,d1}\sum_{i=\pm}\sum_{n=0,1} k^{-i}_{\alpha,n}(k^i_{\alpha,1-n}k^i_{-\alpha,n} + k^{-i}_{-\alpha,n}\sum_j k^j_{-\alpha,n}\delta_{|1+i|,2n}),$$
$$\gamma_1 = \sum_{\alpha=u2,d2}\sum_{i=\pm}\sum_{n=0,1} k^{-i}_{\alpha,n}(k^i_{\alpha,1-n}k^i_{-\alpha,n} + k^{-i}_{-\alpha,n}\sum_j k^j_{-\alpha,n}\delta_{|1+i|,2n}), \tag{11}$$

where $I_{1(2)}$ are the electron number currents through the QD $u1(2)$ [or $d1(2)$], $-u1 = d1$ and $-u2 = d2$, and $k^{i/j}_{\alpha,n}$ are the transition rates (see the Supplemental Material).

Cooling by Thermal Current Effect. In Ref. [58] we have studied the "cooling by transverse heat current" effect, which is a cooling mode in mesoscopic four-terminal thermoelectric devices with two electrodes (the source and the drain) and two heat phononic baths, and the the source can be cooled by driving a heat current between the phononic heat baths. This is different from the previous "cooling by heating" effect where cooling is driven by a photonic heat flow injected into the double-QD quantum system.[33] In the "cooling by thermal current" effect, there is no need to inject the energy into the quantum system because the driving force of refrigeration is the energy exchange between the two heat baths H and C.

We now study the cooling by thermal current effect in the Coulomb coupled QD system, i.e., cooling the source (i.e., $J_{\rm S} > 0$ even though $T_{\rm S} < T_{\rm D}$ and $A_{\rm S} < 0$) as driven by the thermal current J_q when

$$\mu_{\rm S} = \mu_{\rm D} = 0, \quad \text{i.e.,}\ A_{\rm e} = 0, \tag{12a}$$
$$T_{\rm C} = \Big[\frac{2}{T_{\rm D}} - \frac{1}{T_{\rm H}}\Big]^{-1}, \quad \text{i.e.,}\ A_{\rm in} = 0. \tag{12b}$$

We consider the situations with $T_{\rm H} > T_{\rm D} > T_{\rm C}$. $T_{\rm D}$ is the reference temperature that may be set by the substrate. This effect can take place only when $J_q A_q > 0$, i.e., the negative entropy production (i.e., positive free energy production) during the cooling of the source is compensated by the positive entropy production during the thermal conduction J_q (i.e., free energy consumption, $J_q A_q > 0$), so that the total entropy production is non-negative,[55,59]

$$\partial_t S_{\rm tot} = J_q A_q + J_{\rm S}A_{\rm S} \geq 0. \tag{13}$$

The coefficient of performance (COP) for the cooling by thermal current effect is given by the ratio of the two heat currents

$$\eta_{\rm COP} = \frac{J_{\rm S}}{J_q} = \frac{E_{u1}I_1 + (E_{u2}+E_{\rm C})I_2}{\Big(E_{d1}+\frac{1}{2}E_{\rm C}\Big)I_1 + \Big(E_{d2}+\frac{1}{2}E_{\rm C}\Big)I_2}. \tag{14}$$

From Eq. (13) and the definition of the COP we find that the reversible COP is

$$\eta^{\rm rev}_{\rm COP} = \Big(\frac{T_{\rm S}}{T_{\rm C}} - \frac{T_{\rm S}}{T_{\rm H}}\Big)\frac{T_{\rm D}}{T_{\rm D}-T_{\rm S}} = -\frac{A_q}{A_{\rm S}}. \tag{15}$$

We regard $T_{\rm D}$ as the reference temperature fixed by the substrate and $T_{\rm C}$ as determined by Eq. (12b), so that only the temperatures $T_{\rm S}$ and $T_{\rm H}$ are independent variables. The working condition for the cooling driven by the thermal current J_q is restricted by

$$0 \leq \eta_{\rm COP} \leq -\frac{A_q}{A_{\rm S}}. \tag{16}$$

At reversible COP $\eta^{\rm rev}_{\rm COP} = -\frac{A_q}{A_{\rm S}}$ the cooling power vanishes, since the entropy production and the currents vanish.[55,59,60]

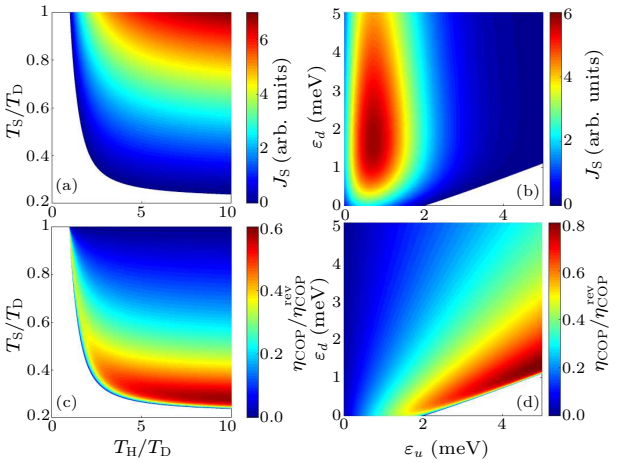

Fig. 3. (a) Cooling power $J_{\rm S}$ as functions of temperature ratios $T_{\rm S}/T_{\rm D}$ and $T_{\rm H}/T_{\rm D}$ for $E_{u1} = E_{u2} = E_{d1} = E_{d2} = 1$ meV. (b) Cooling power $J_{\rm S}$ as functions of QDs energies $E_{u1} = E_{u2} = \varepsilon_u$ and $E_{d1} = E_{d2} = \varepsilon_d$ for $k_{\rm B}T_{\rm H} = 6$ meV and $k_{\rm B}T_{\rm S} = 0.6$ meV. (c) The COP ratio $\eta_{\rm COP}/\eta^{\rm rev}_{\rm COP}$ for the cooling by thermal current effect as functions of the temperature ratios $T_{\rm S}/T_{\rm D}$ and $T_{\rm H}/T_{\rm D}$ when QDs energy is the same as in (a). (d) $\eta_{\rm COP}/\eta^{\rm rev}_{\rm COP}$ as functions of QDs energies ε_u and ε_d for the same parameters as in (b). Common parameters: $\mu_{\rm S} = \mu_{\rm D} = 0$, $k_{\rm B}T_{\rm D} = 1$ meV, $T_{\rm C} = 1/(2/T_{\rm D} - 1/T_{\rm H})$, $\Gamma_0 = 0.1$ meV, and $E_{\rm C} = 2$ meV. The white areas represent the parameter regions where the cooling by thermal current cannot be achieved, i.e., $J_{\rm S} < 0$.

In Fig. 3(a) the cooling power of our nonelectric refrigerator is large when the temperature of the source

T_S is close to the temperature of drain T_D and when the temperature of the heat bath T_H is much higher than the temperature of the drain, $T_H \gg T_D$. From Fig. 3(a) the lowest temperature of the source T_S that can be cooled down is about $0.25T_D$. In the white region the device cannot function as a refrigerator. As shown in Fig. 3(b), for a given temperature of $T_H = 6T_D$ and $T_S = 0.6T_D$, the cooling power is large for $E_{u1} = E_{u2} = \varepsilon_u$ around k_BT_D ($k_BT_D = 1$ meV throughout this paper), particularly when $\varepsilon_d \gtrsim \varepsilon_u$. In Fig. 3(c) the ratio of the COP over the reversible COP $\eta_{COP}/\eta_{COP}^{rev}$ is high when the temperature of the source T_S is low. This is the regime where the cooling power is rather low. Similarly, as shown in Fig. 3(d), the COP ratio $\eta_{COP}/\eta_{COP}^{rev}$ is high when ε_d is small, where the cooling power is very low. The COP can be quite a considerable fraction of the reversible COP, indicating that the coupling is strong and the dissipation is low for such optimized efficiency conditions.[60] This phenomenon that the efficiency is optimized when the output power is low (for small dissipations), known as the efficiency-power trade-off, is consistent with the literature available.[55,60,61]

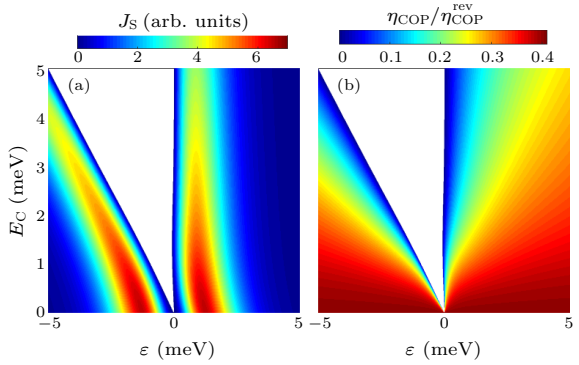

Fig. 4. (a) Cooling power J_S and (b) COP ratio $\eta_{COP}/\eta_{COP}^{rev}$ as functions of the QDs energies $E_{u1} = E_{u2} = E_{d1} = E_{d2} = \varepsilon$ and E_C. Other parameters: $\mu_S = \mu_D = 0$, $k_BT_D = 1$ meV, $k_BT_H = 6$ meV, $k_BT_S = 0.6$ meV, $T_C = 1/(2/T_D - 1/T_H)$, and $\Gamma_0 = 0.1$ meV.

We now study more on the QDs energy dependence of the cooling power J_S and the COP ratio $\eta_{COP}/\eta_{COP}^{rev}$ for several different configurations. We first consider the case with $E_{u1} = E_{u2} = E_{d1} = E_{d2} = \varepsilon$ and study how the energy ε and the charge interaction energy E_C affect the power and the COP. First, the cooling by thermal current effect holds for all $E_C > 0$ when $\varepsilon > 0$. However, as shown in Fig. 4(a), for $\varepsilon < 0$, the cooling by thermal current effect holds only when $E_C < -\varepsilon$. This is due to $M_{S,q} = e^{-2}TG[p_1\varepsilon(\varepsilon + \frac{1}{2}E_C) + p_2(\varepsilon + E_C)(\varepsilon + \frac{1}{2}E_C)]$ in this regime. The condition for positive $M_{S,q}$ holds when $E_C < -\varepsilon$. From Figs. 4(a) and 4(b), we note that the optimal parameters for both COP and cooling power can be $\varepsilon \sim k_BT_D$ and $E_C \sim k_BT_D$, or $\varepsilon \sim -2k_BT_D$ and $E_C \sim k_BT_D$ ($k_BT_D = 1$ meV). Although the COP ratio increases with decreasing E_C for any given ε, the limit with $E_C \to 0$ does not validate our theory.

Four-Terminal Thermoelectric System as a Maxwell's Demon. Maxwell's demon is a hypothetical demon, which can detect and control the motion of a single molecule. It was conceived by James Clerk Maxwell in 1871 to explain the possibility of violating the second law of thermodynamics. The demon is assumed to control a door, which separates two boxes to realize the non-equilibrium gas distribution.[62] This operation that appeared to be in violation of the second law of thermodynamics, decreasing the entropy of the gas without any work input. Despite the complexity, such a Maxwell's demon has been realized in various systems in different forms.[63–66] For example, the QD multi-terminal systems can be possibly realized as a Maxwell's demon using the inelastic transport without any measurement of individual particles or any feedback involved.[50,58,67,68]

As shown in Fig. 5, here we introduce a Maxwell's demon based on two electronic thermal baths (the hot bath H and cold bath C) which can reduce the entropy of the working substance (the source and the drain), without changing the energies and particles of the working substance. The nonequilibrium Maxwell's demon is used to reverse the natural direction of the source and drain where the drain has a higher temperature. As we introduced in the previous section, when we realize the cooling by thermal current effect, the entropy of the source and drain is reduced, while the entropy of the whole thermoelectric system is increased. This operation seemingly break the the second law of thermodynamics, the entropy production of the two heat baths H and C compensates for that of the source and drain.

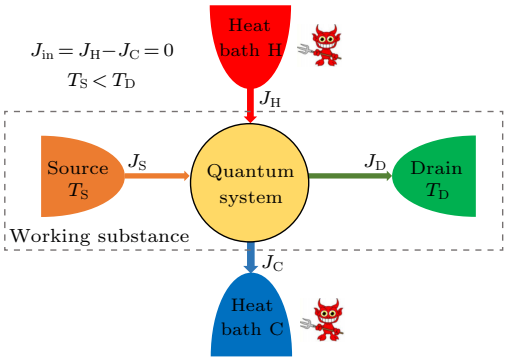

Fig. 5. Illustration of a four-terminal mesoscopic thermoelectric device as a Maxwell demon. Maxwell's demon does not supply any energy to the working substance, i.e., the total heat current injected into the central quantum system from the two thermal baths is zero, $J_{in} = J_H - J_C = 0$.

The condition at which Maxwell's demon neither injects nor extracts heat or energy into the working substance is[58]

$$J_{in} = 0. \tag{17}$$

The power of the Maxwell demon vanishes when the temperature gradient between the two heat baths H and C is vanishing.

In Fig. 6, we show that in our system it is indeed able to realize the cooling by thermal current with vanishing total injected heat, $J_{\rm in} = 0$. We find that the cooling by thermal current effect emerges in the whole region of $0 \leq \varepsilon_2 \leq 5\,{\rm meV}$, regardless of the sign change and the vanishing of the total heat injected into the QDs $u1$ and $d1$ from the two heat baths H and C. From the illustration in Fig. 6(b), we can find that $J_{\rm S}A_{\rm S}$ is negative and J_qA_q is positive when $\varepsilon_2 \approx 2.1$ meV, i.e., $J_{\rm in} = 0$. Therefore, the entropy of the whole system is still increasing, and the entropy decrease of the working substance is compensated by the entropy increase of the two heat baths. This results are consistent with Ref. [58].

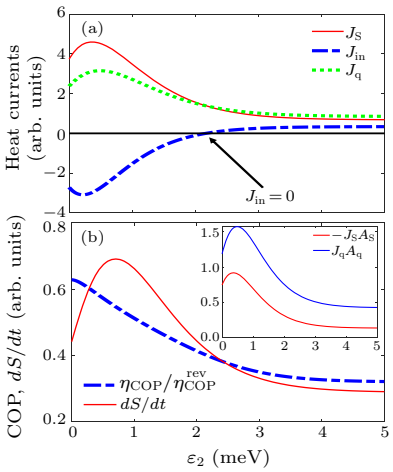

Fig. 6. (a) Cooling power $J_{\rm S}$, the total injected heat $J_{\rm in}$, and the thermal current J_q as a function of the QD energy $E_{u2} = E_{d2} = \varepsilon_2$. (b) COP ratio $\eta_{\rm COP}/\eta_{\rm COP}^{\rm rev}$, entropy production rate $\partial_t S_{\rm tot}$ as a function of the QDs energy $E_{u2} = E_{d2} = \varepsilon_2$. Inset: $-J_{\rm S}A_{\rm S}$, J_qA_q as a function of the QDs energy ε_2. Other parameters: $\mu_{\rm S} = \mu_{\rm D} = 0$, $k_{\rm B}T_{\rm D} = 1\,{\rm meV}$, $k_{\rm B}T_{\rm H} = 6\,{\rm meV}$, $k_{\rm B}T_{\rm S} = 0.6\,{\rm meV}$, $T_{\rm C} = 1/(2/T_{\rm D} - 1/T_{\rm H})$, $E_{u1} = E_{d1} = \varepsilon_1 = 4\,{\rm meV}$, $E_{\rm C} = 2\,{\rm meV}$, and $\Gamma_0 = 0.1\,{\rm meV}$.

Conclusion and Discussions. In this work, we have demonstrated a mode of the cooling by thermal current effect, the transverse thermoelectric effect and Maxwell's demon effect, through a four-terminal four QDs thermoelectric device (the four terminals are the source, the drain and two electronic thermal baths, respectively). We have demonstrated that the Coulomb interaction between the two circuits separated by an insulating layer is the key factor and the inelastic thermoelectric transport in the two circuits leads to these three unconventional thermoelectric effects. The source can be cooled by passing a thermal current between the two electronic heat baths.

We have also shown that the two thermal baths can be exploited for power generation and cooling the low-temperature heat bath (or heating the high-temperature heat bath) in a demon-like way, where the working substance does not exchange any energy or particle with the two thermal baths. Our study may be beneficial for autonomous and energy-efficient electric applications on the nanoscale devices.

The authors thank Professor Chen Wang for helpful discussion.

References

[1] Chen G 2005 *Nanoscale Energy Transport and Conversion* (Oxford: Oxford University Press)
[2] Dubi Y and Di Ventra M 2011 *Rev. Mod. Phys.* **83** 131
[3] Jiang J H and Imry Y 2016 *C. R. Phys.* **17** 1047
[4] Benenti G, Casati G, Saito K and Whitney R S 2017 *Phys. Rep.* **694** 1
[5] Sivan U and Imry Y 1986 *Phys. Rev. B* **33** 551
[6] Mahan G D and Sofo J O 1996 *Proc. Natl. Acad. Sci. USA* **93** 7436
[7] Goldsmid H J 2010 *Introduction to Thermoelectricity* (Berlin: Springer)
[8] Venkatasubramanian R, Silvola E, Colpitts T and O'Quinn B 2001 *Nature* **413** 597
[9] Jiang J H, Weng M Q and Wu M W 2006 *J. Appl. Phys.* **100** 063709
[10] Humphrey T E and Linke H 2005 *Phys. Rev. Lett.* **94** 096601
[11] Zhou J, Yang R, Chen G and Dresselhaus M S 2011 *Phys. Rev. Lett.* **107** 226601
[12] Lu J, Wang R, Liu Y and Jiang J H 2017 *J. Appl. Phys.* **122** 044301
[13] Lin Z, Yang Y Y, Li W, Wang J and He J 2020 *Phys. Rev. E* **101** 022117
[14] Sánchez R and Büttiker M 2011 *Phys. Rev. B* **83** 085428
[15] Sánchez D and López R 2013 *Phys. Rev. Lett.* **110** 026804
[16] Simine L and Segal D 2012 *Phys. Chem. Chem. Phys.* **14** 13820
[17] Jiang J H, Entin-Wohlman O and Imry Y 2012 *Phys. Rev. B* **85** 075412
[18] Jordan A N, Sothmann B, Sánchez R and Büttiker M 2013 *Phys. Rev. B* **87** 075312
[19] Sothmann B, Sánchez R and Jordan A N 2015 *Nanotechnology* **26** 032001
[20] Li L and Jiang J H 2016 *Sci. Rep.* **6** 31974
[21] Agarwalla B K, Jiang J H and Segal D 2017 *Phys. Rev. B* **96** 104304
[22] Wang R, Lu J, Wang C and Jiang J H 2018 *Sci. Rep.* **8** 2607
[23] Jiang J H and Imry Y 2017 *Phys. Rev. Appl.* **7** 064001
[24] Jiang J H and Imry Y 2018 *Phys. Rev. B* **97** 125422
[25] Erdman P A, Bhandari B, Fazio R, Pekola J P and Taddei F 2018 *Phys. Rev. B* **98** 045433
[26] Bhandari B, Chiriacò G, Erdman P A, Fazio R and Taddei F 2018 *Phys. Rev. B* **98** 035415
[27] Lu J, Wang R, Ren J, Kulkarni M and Jiang J H 2019 *Phys. Rev. B* **99** 035129
[28] Prete D, Erdman P A, Demontis V, Zannier V, Ercolani D, Sorba L, Beltram F, Rossella F, Taddei F and Roddaro S 2019 *Nano Lett.* **19** 3033
[29] Jaliel G, Puddy R K, Sánchez R, Jordan A N, Sothmann B, Farrer I, Griffiths J P, Ritchie D A and Smith C G 2019 *Phys. Rev. Lett.* **123** 117701
[30] Sothmann B, Sánchez R, Jordan A N and Büttiker M 2012 *Phys. Rev. B* **85** 205301
[31] Jiang J H 2014 *J. Appl. Phys.* **116** 194303

[32] Mari A and Eisert J 2012 *Phys. Rev. Lett.* **108** 120602
[33] Cleuren B, Rutten B and van den Broeck C 2012 *Phys. Rev. Lett.* **108** 120603
[34] Lu J, Wang R, Wang C and Jiang J H 2020 *Phys. Rev. B* **102** 125405
[35] Li B, Wang L and Casati G 2004 *Phys. Rev. Lett.* **93** 184301
[36] Li B, Wang L and Casati G 2006 *Appl. Phys. Lett.* **88** 143501
[37] Jiang J H, Kulkarni M, Segal D and Imry Y 2015 *Phys. Rev. B* **92** 045309
[38] Joulain K, Drevillon J, Ezzahri Y and Ordonez-Miranda J 2016 *Phys. Rev. Lett.* **116** 200601
[39] Sánchez R, Thierschmann H and Molenkamp L W 2017 *Phys. Rev. B* **95** 241401
[40] Entin-Wohlman O, Imry Y and Aharony A 2010 *Phys. Rev. B* **82** 115314
[41] Ren J, Zhu J X, Gubernatis J E, Wang C and Li B 2012 *Phys. Rev. B* **85** 155443
[42] Jiang J H, Entin-Wohlman O and Imry Y 2013 *Phys. Rev. B* **87** 205420
[43] Agarwalla B K, Jiang J H and Segal D 2015 *Phys. Rev. B* **92** 245418
[44] Narozhny B N and Levchenko A 2016 *Rev. Mod. Phys.* **88** 025003
[45] Sánchez R, López R, Sánchez D and Büttiker M 2010 *Phys. Rev. Lett.* **104** 076801
[46] Hartmann F, Pfeffer P, Höfling S, Kamp M and Worschech L 2015 *Phys. Rev. Lett.* **114** 146805
[47] Zhang Y, Lin G and Chen J 2015 *Phys. Rev. E* **91** 052118
[48] Thierschmann H, Sánchez R, Sothmann B, Buhmann H and Molenkamp L W 2016 *C. R. Phys.* **17** 1109
[49] Yang J, Elouard C, Splettstoesser J, Sothmann B, Sánchez R and Jordan A N 2019 *Phys. Rev. B* **100** 045418
[50] Sánchez R, Samuelsson P and Potts P P 2019 *Phys. Rev. Res.* **1** 033066
[51] He W X, Cao Z, Li G Y, Li L, Lü H F, Li Z and Luo H G 2020 *Phys. Rev. B* **101** 035417
[52] Tabatabaei S M, Sanchez D, Yeyati A L and Sanchez R 2020 *Phys. Rev. Lett.* **125** 247701
[53] Sánchez R, Sothmann B, Jordan A N and Bttiker M 2013 *New J. Phys.* **15** 125001
[54] Whitney R S, Sánchez R, Haupt F and Splettstoesser J 2016 *Physica E* **75** 257
[55] Jiang J H 2014 *Phys. Rev. E* **90** 042126
[56] Jiang J H, Agarwalla B K and Segal D 2015 *Phys. Rev. Lett.* **115** 040601
[57] Proesmans K, Cleuren B and van den Broeck C 2016 *Phys. Rev. Lett.* **116** 220601
[58] Lu J, Jiang J H and Imry Y 2021 *Phys. Rev. B* **103** 085429
[59] Kedem O and Caplan S R 1965 *Trans. Faraday Soc.* **61** 1897
[60] Entin-Wohlman O, Jiang J H and Imry Y 2014 *Phys. Rev. E* **89** 012123
[61] Lu J, Liu Y, Wang R, Wang C and Jiang J H 2019 *Phys. Rev. B* **100** 115438
[62] Maxwell J C 1871 *Theory of Heat* (London: Longman)
[63] Koski J V, Maisi V F, Sagawa T and Pekola J P 2014 *Phys. Rev. Lett.* **113** 030601
[64] Koski J V, Kutvonen A, Khaymovich I M, Ala-Nissila T and Pekola J P 2015 *Phys. Rev. Lett.* **115** 260602
[65] Koski J V, Maisi V F, Pekola J P and Averin D V 2014 *Proc. Natl. Acad. Sci. USA* **111** 13786
[66] Chida K, Desai S, Nishiguchi K and Fujiwara A 2017 *Nat. Commun.* **8** 15310
[67] Sánchez R, Splettstoesser J and Whitney R S 2019 *Phys. Rev. Lett.* **123** 216801
[68] Annby-Andersson B, Samuelsson P, Maisi V F and Potts P P 2020 *Phys. Rev. B* **101** 165404

Supplemental Material: Coulomb thermoelectric drag in four-terminal mesoscopic quantum transport

Mengmeng Xi(席萌萌)[1], Rongqian Wang(王荣倩)[2],
Jincheng Lu(陆金成)[3,2]*, and Jian-Hua Jiang(蒋建华)[2]†
[1] Hefei National Laboratory for Physical Sciences at Microscale,
University of Science and Technology of China, Hefei, 230026, China
[2] School of physical science and technology and Collaborative Innovation Center
of Suzhou Nano Science and Technology, Soochow University, Suzhou 215006, China.
[3] Center for Phononics and Thermal Energy Science, China-EU Joint Lab on Nanophononics,
Shanghai Key Laboratory of Special Artificial Microstructure Materials and Technology,
School of Physics Science and Engineering, Tongji University, Shanghai 200092 China

June 8, 2021

1. Derivation of the expressions of the currents

1.1. Double quantum-dots thermoelectric systems

We now study the steady-state transport through $u1$ and $d1$ using the master equation method as in Ref. [1]. There are four quantum states for electrons in the two QDs $u1$ and $d1$, respectively, characterized by the quantum numbers n_{u1} and n_{d1}, and denoted as $|n_{u1}, n_{d1}\rangle$. The electron density matrix of the QDs system at the steady-state is characterized by the four-component vector $\rho = (\rho_{0,0}, \rho_{1,0}, \rho_{0,1}, \rho_{1,1})^T$. The steady-state transport currents are determined by the steady-state density matrix ρ, which is obtained by solving the master equation for steady-state, $\partial_t \rho = \hat{L}_{(1)}\rho = 0$. Here

$$\hat{L}_{(1)} = \begin{pmatrix} -k^+_{u1,0} - k^+_{d1,0} & k^-_{u1,0} & k^-_{d1,0} & 0 \\ k^+_{u1,0} & -k^-_{u1,0} - k^+_{d1,1} & 0 & k^-_{d1,1} \\ k^+_{d1,0} & 0 & -k^-_{d1,0} - k^+_{u1,1} & k^-_{u1,1} \\ 0 & k^+_{d1,1} & k^+_{u1,1} & -k^-_{d1,1} - k^-_{u1,1} \end{pmatrix} \tag{1}$$

*Corresponding author. E-mail: jincheng.lu1993@gmail.com
†Corresponding author. E-mail: jianhuajiang@suda.edu.cn

The transition rates are

$$k^{\pm}_{u1,n_{d1}} \equiv k^{\pm}_{S,u1,n_{d1}} + k^{\pm}_{D,u1,n_{d1}}, \tag{2a}$$

$$k^{\pm}_{d1,n_{u1}} \equiv k^{\pm}_{H,d1,n_{u1}} + k^{\pm}_{C,d1,n_{u1}}, \tag{2b}$$

where the superscript $+$ $(-)$ representing the rates for the processes with electron entering into (leaving) the QD. For the "k" in the right hand sides of the equations, the first two subscripts denote the reservoir and the QD as the starting or end point of the tunneling, while the third subscript denotes the number of electrons in the capacitively coupled QD (e.g., for tunneling into the QD $u1$, the capacitively coupled QD is $d1$). And

$$k^{+}_{i,u1,n_{d1}} \equiv \Gamma_{i,u1,n_{d1}} f\left(\frac{E_{u1,n_{d1}} - \mu_i}{k_B T_i}\right), \quad i = S, D, \tag{3a}$$

$$k^{+}_{i,d1,n_{u1}} \equiv \Gamma_{i,d1,n_{u1}} f\left(\frac{E_{d1,n_{u1}}}{k_B T_i}\right), \quad i = H, C, \tag{3b}$$

$$k^{-}_{i,u1,n_{d1}} \equiv \Gamma_{i,u1,n_{d1}} - k^{+}_{i,u1,n_{d1}}, \quad i = S, D, \tag{3c}$$

$$k^{-}_{i,d1,n_{u1}} \equiv \Gamma_{i,d1,n_{u1}} - k^{+}_{i,d1,n_{u1}}, \quad i = H, C, \tag{3d}$$

where $\Gamma_{i,u1,n_{d1}}$ is the tunneling rate between the reservoir i and the QD $u1$ at energy $E_{u1,n_{d1}}$ (the other tunneling rates are defined similarly), and $f(x) = 1/(e^x + 1)$ is the Fermi-Dirac distribution function.

In the above equations, we have set

$$\mu_H = \mu_C \equiv 0 \tag{4}$$

as both the equilibrium electrochemical potential and the energy zero for electrons. The tunneling rates can, in principle, be calculated via the Fermi golden rule [2,3]. In this work, however, we assume that they can be tuned at will in experiments (e.g., by changing the channel width of the leads, or attaching QDs that are strongly coupled with the leads; in the former we change the step-function like tunneling rates, while in the latter Lorentzian shape tunneling rates can be formed). It has been found that asymmetry in the tunneling rates Γ_i (as functions of energy) is crucial to induce inelastic thermoelectric transport in the QDs system.

1.2. Four quantum-dots thermoelectric system

Transport equations through the other pair of QDs, $u2$ and $d2$, can be solved similarly. In fact, the matrix $\hat{L}_{(2)}$ is the same as $\hat{L}_{(1)}$ with only $u1$ replaced by $u2$ and $d1$ replaced by $d2$. We shall use the vector $\rho' = (\rho'_{0,0}, \rho'_{1,0}, \rho'_{0,1}, \rho'_{1,1})^T$ to represent the density matrix of electrons in the QDs $u2$ and $d2$ at the transport steady-state. Here each element of the density matrix $\rho'_{n_{u2}n_{d2}}$ carries the index characterizing the quantum states of electrons in the QDs $u2$ and $d2$, $|n_{u2}, n_{d2}\rangle$.

After numerically solving the master equations at the steady-state transport [1,4]

$$\hat{L}_{(1)}\rho = 0, \quad \hat{L}_{(2)}\rho' = 0, \tag{5}$$

one can determine the steady-state transport currents from ρ and ρ' as,

$$\rho_{00} = \gamma^{-3} \sum_{\alpha=u1,d1} \sum_{i=\pm1} \sum_{n=0,1} \Gamma^{-}_{\alpha 0}\Gamma^{i}_{\alpha 1}\Gamma^{-}_{\bar{l}n}\delta_{|1-i|,2n}, \tag{6a}$$

$$\rho_{10} = \gamma^{-3} \sum_{i=\pm1} \sum_{n=0,1} \left(\Gamma^{+}_{u1,0}\Gamma^{i}_{u1,1}\Gamma^{-}_{d1,n} + \Gamma^{i}_{d1,0}\Gamma^{-}_{d1,1}\Gamma^{+}_{u1,n}\right)\delta_{|1-i|,2n}, \tag{6b}$$

$$\rho_{01} = \gamma^{-3} \sum_{i=\pm1} \sum_{n=0,1} \left(\Gamma^{i}_{u1,0}\Gamma^{-}_{u1,1}\Gamma^{+}_{d1,n} + \Gamma^{+}_{d1,0}\Gamma^{i}_{d1,1}\Gamma^{-}_{u1,n}\right)\delta_{|1-i|,2n}, \tag{6c}$$

$$\rho_{11} = \gamma^{-3} \sum_{\alpha=u1,d1} \sum_{i=\pm1} \sum_{n=0,1} \Gamma^{i}_{\alpha 0}\Gamma^{+}_{\alpha 1}\Gamma^{+}_{\bar{\alpha}n}\delta_{|1-i|,2n}. \tag{6d}$$

with $\gamma^3 = \sum_{\alpha i n} \Gamma^{i}_{\alpha n}\left(\Gamma^{\bar{i}}_{\alpha\bar{n}}\Gamma^{\bar{i}}_{\bar{\alpha}n} + \Gamma^{i}_{\bar{\alpha}n}\sum_j \Gamma^{j}_{\bar{\alpha}n}\delta_{|1-i|,2n}\right)$ satisfying the normalization condition $\sum_i \rho_{ii} = 1$. The indices with a bar on top denote an opposite value, for example: $\bar{u}1 = d1$, $\bar{0} = 1$. Similarly, we also can obtain the expressions of ρ'_{ii}. The currents read

$$J_e = \sum_{n_{d1}} e(k^{+}_{S,u1,n_{d1}}\rho_{0,n_{d1}} - k^{-}_{S,u1,n_{d1}}\rho_{1,n_{d1}}) + \sum_{n_{d2}} e(k^{+}_{S,u2,n_{d2}}\rho'_{0,n_{d2}} - k^{-}_{S,u2,n_{d2}}\rho'_{1,n_{d2}}), \tag{7a}$$

$$J_S = \sum_{n_{d1}} (E_{u1,n_{d1}} - \mu_S)(k^{+}_{S,u1,n_{d1}}\rho_{0,n_{d1}} - k^{-}_{S,u1,n_{d1}}\rho_{1,n_{d1}}) + \sum_{n_{d2}} (E_{u2,n_{d2}} - \mu_S)(k^{+}_{S,u2,n_{d2}}\rho'_{0,n_{d2}} - k^{-}_{S,u2,n_{d2}}\rho'_{1,n_{d2}}), \tag{7b}$$

$$J_H = \sum_{n_{u1}} E_{d1,n_{u1}}(k^{+}_{H,d1,n_{u1}}\rho_{n_{u1},0} - k^{-}_{H,d1,n_{u1}}\rho_{n_{u1},1}) + \sum_{n_{u2}} E_{d2,n_{u2}}(k^{+}_{H,d2,n_{u2}}\rho'_{n_{u2},0} - k^{-}_{H,d2,n_{u2}}\rho'_{n_{u2},1}), \tag{7c}$$

$$J_C = \sum_{n_{u1}} E_{d1,n_{u1}}(k^{-}_{C,d1,n_{u1}}\rho_{n_{u1},1} - k^{+}_{C,d1,n_{u1}}\rho_{n_{u1},0}) + \sum_{n_{u2}} E_{d2,n_{u2}}(k^{-}_{C,d2,n_{u2}}\rho'_{n_{u2},1} - k^{+}_{C,d2,n_{u2}}\rho'_{n_{u2},0}). \tag{7d}$$

We can obtain J_{in} and J_q from the two currents, J_H and J_C.

1.3. Inelastic thermoelectric transport through correlated tunneling

We now study a special configuration that allows unconventional thermoelectric transport through drag effects. In this configuration, we choose the following tunneling rates,

$$\begin{aligned}
&\Gamma_{S,u1,n_{d1}=0} = \Gamma_0, \quad \Gamma_{S,u1,n_{d1}=1} = 0,\\
&\Gamma_{D,u1,n_{d1}=0} = 0, \quad \Gamma_{D,u1,n_{d1}=1} = \Gamma_0,\\
&\Gamma_{H,d1,n_{u1}=0} = 0, \quad \Gamma_{H,d1,n_{u1}=1} = \Gamma_0,\\
&\Gamma_{C,d1,n_{u1}=0} = \Gamma_0, \quad \Gamma_{C,d1,n_{u1}=1} = 0;\\
&\Gamma_{S,u2,n_{d2}=0} = 0, \quad \Gamma_{S,u2,n_{d2}=1} = \Gamma_0,\\
&\Gamma_{D,u2,n_{d2}=0} = \Gamma_0, \quad \Gamma_{D,u2,n_{d2}=1} = 0,\\
&\Gamma_{H,d2,n_{u2}=0} = \Gamma_0, \quad \Gamma_{H,d2,n_{u2}=1} = 0,\\
&\Gamma_{C,d2,n_{u2}=0} = 0, \quad \Gamma_{C,d2,n_{u2}=1} = \Gamma_0,
\end{aligned} \tag{8}$$

where Γ_0 is a constant for the tunneling rates. The above configuration is schematically illustrated in Fig. 3(a) and Fig. 3(b) in the main text. For such a configuration, in the QDs $u1$ and $d1$ only the following process of

electron motion (and its time-reversal) is possible,

$$|0,0\rangle \xrightarrow[QD\ u1:\ E_{u1}]{\Gamma_{S,u1,0}} |1,0\rangle \xrightarrow[QD\ d1:\ E_{d1}+E_C]{\Gamma_{H,d1,1}} |1,1\rangle \xrightarrow[QD\ u1:\ E_{u1}+E_C]{\Gamma_{D,u1,1}} |0,1\rangle \xrightarrow[QD\ d1:\ E_{d1}]{\Gamma_{C,d1,0}} |0,0\rangle. \tag{9}$$

The above expression represents the correlated electron tunneling through the QDs $u1$ and $d1$. The quantum states are labeled by the two integers n_{u1}, n_{d1}. In the above expression, below each arrow is the QD of which electron is tunneling into or outside and the energy of the electron that tunnels, while above each arrow is the tunneling rate. The consequence of the above correlated tunneling processes is an electron traverses from the H reservoir to the C reservoir via the QD $d1$, in the meanwhile an electron traverses from the source to the drain via the QD $u1$. The interaction between the electrons in the two QDs provides the mechanism for passing energy between the two channels. The electron traverse from H to C loses energy E_C, while the electron traverses from the source to the drain and gains energy E_C. The above correlated tunneling processes, as the only passage for electron transport through the QDs $u1$ and $d1$, also dictates the direction correlation between the electron flowing in the two channels: when an electron goes from H to C, there has to be an electron moving from the source to the drain, otherwise the energy is not conserved! Such locking between electron motions in the two channels is the key for the unconventional thermoelectric transport in our system.

Similarly, for transport through the QDs $u2$ and $d2$, only the following process and its time-reversal is allowed,

$$|0,0\rangle \xrightarrow[QD\ d2:\ E_{d2}]{\Gamma_{H,d2,0}} |0,1\rangle \xrightarrow[QD\ u2:\ E_{u2}+E_C]{\Gamma_{S,u2,1}} |1,1\rangle \xrightarrow[QD\ d2:\ E_{d2}+E_C]{\Gamma_{C,d2,1}} |1,0\rangle \xrightarrow[QD\ u2:\ E_{u2}]{\Gamma_{D,u2,0}} |0,0\rangle. \tag{10}$$

Each time the above process (the reversed process) takes place, an electron traverse from H to C, and another electron traverse from the source to the drain. There are always an equal number of electrons traveling from H to C as the number of electrons traveling from the source to the drain.

According to the above picture, the electrical and heat currents can be expressed as

$$J_e = e\sum I_i, \tag{11a}$$

$$J_S = E_{u1}I_1 + (E_{u2}+E_C)I_2, \tag{11b}$$

$$J_H = (E_{d1}+E_C)I_1 + E_{d2}I_2, \tag{11c}$$

$$J_C = E_{d1}I_1 + (E_{d2}+E_C)I_2, \tag{11d}$$

$$J_{in} = E_C(I_1 - I_2), \tag{11e}$$

$$J_q = (E_{d1}+\frac{1}{2}E_C)I_1 + (E_{d2}+\frac{1}{2}E_C)I_2, \tag{11f}$$

where

$$I_1 = \gamma_1^{-1}(k^+_{u1,0}k^+_{d1,1}k^-_{u1,1}k^-_{d1,0} - k^+_{d1,0}k^+_{u1,1}k^-_{d1,1}k^-_{u1,0}), \tag{12a}$$

$$I_2 = \gamma_2^{-1}(k^+_{d2,0}k^+_{u2,1}k^-_{d2,1}k^-_{u2,0} - k^+_{u2,0}k^+_{d2,1}k^-_{u2,1}k^-_{d2,0}), \tag{12b}$$

are the electron number current through the QD $u1$ (or $d1$), and the electron number current through the QD $u2$ (or $d2$), respectively. According to Ref. [1],

$$\begin{aligned}
\gamma_1 &= \sum_{\alpha=u1,d1}\sum_{i=\pm}\sum_{n=0,1} k^{-i}_{\alpha,n}(k^i_{\alpha,1-n}k^i_{-\alpha,n} + k^{-i}_{-\alpha,n}\sum_j k^j_{-\alpha,n}\delta_{|1+i|,2n}),\\
\gamma_1 &= \sum_{\alpha=u2,d2}\sum_{i=\pm}\sum_{n=0,1} k^{-i}_{\alpha,n}(k^i_{\alpha,1-n}k^i_{-\alpha,n} + k^{-i}_{-\alpha,n}\sum_j k^j_{-\alpha,n}\delta_{|1+i|,2n}),
\end{aligned} \tag{13}$$

where $-u1 = d1$ and $-u2 = d2$.

2. Unconventional Thermoelectric energy conversion

From the relations between currents we can also obtain the relations between the linear-response transport coefficients. If $I_i = \sum_j M_{ij} A_j$ $(i, j = e, S, in, q)$ where M_{ij} are the linear-response transport coefficients, then

$$M_{e,e} = TG, \quad M_{e,S} = e^{-1}TG\left[p_1 E_{u1} + p_2(E_{u2} + E_C)\right], \quad M_{e,in} = e^{-1}TGE_C(p_1 - p_2), \tag{14a}$$

$$M_{e,q} = e^{-1}TG\left[p_1 E_{d1} + p_2 E_{d2} + \frac{1}{2}E_C\right], \quad M_{S,S} = e^{-2}TG\left[p_1 E_{u1}^2 + p_2(E_{u2} + E_C)^2\right], \tag{14b}$$

$$M_{S,in} = e^{-2}TG\left[p_1 E_{u1} E_C - p_2(E_{u2} + E_C)E_C\right], \tag{14c}$$

$$M_{S,q} = e^{-2}TG\left[p_1 E_{u1}(E_{d1} + \frac{1}{2}E_C) + p_2(E_{u2} + E_C)(E_{d2} + \frac{1}{2}E_C)\right], \tag{14d}$$

$$M_{in,in} = e^{-2}TGE_C^2, \quad M_{in,q} = e^{-2}TG\left[p_1 E_C(E_{d1} + \frac{1}{2}E_C) - p_2 E_C(E_{d2} + \frac{1}{2}E_C)\right], \tag{14e}$$

$$M_{q,q} = e^{-2}TG\left[p_1(E_{d1} + \frac{1}{2}E_C)^2 + p_2(E_{d2} + \frac{1}{2}E_C)^2\right] \tag{14f}$$

where G is the total conductance, and $p_i = G_i/G$ $(i = 1, 2)$ with G_i being the conductance for the transport through the QDs pair $u1$ and $d1$ (if $i = 1$) or that for the transport through the QDs pair $u2$ and $d2$ (if $i = 2$).

There are three different types of thermoelectric effects, associated with the following Seebeck coefficients,

$$S_S = \frac{M_{e,S}}{T^2 G} = \frac{k_B}{e}\frac{\langle a_S\rangle}{k_B T}, \tag{15a}$$

$$S_{in} = \frac{M_{e,in}}{T^2 G} = \frac{k_B}{e}\frac{\langle a_{in}\rangle}{k_B T}, \tag{15b}$$

$$S_q = \frac{M_{e,q}}{T^2 G} = \frac{k_B}{e}\frac{\langle a_q\rangle}{k_B T}, \tag{15c}$$

where

$$\langle\mathcal{O}\rangle = \sum_{i=1,2} p_i \mathcal{O}_i \tag{16a}$$

$$a_{S,1} = E_{u1}, \quad a_{S,2} = E_{u2} + E_C, \tag{16b}$$

$$a_{in,1} = E_C, \quad a_{in,2} = -E_C, \tag{16c}$$

$$a_{q,1} = E_{d1} + \frac{1}{2}E_C, \quad a_{q,2} = E_{d2} + \frac{1}{2}E_C. \tag{16d}$$

In our system which breaks the left-right inversion symmetry and up-down inversion symmetry [see Eq. (8)], if $p_1 = p_2$, the Seebeck coefficient S_{in} vanishes. The other two Seebeck coefficients are nonzero even at the particle-hole symmetric limit with $E_{u1} = E_{d1} = E_{u2} = E_{d2} = 0$. The figures of merit for these three thermoelectric effects can be expressed as

$$Z_S T = \frac{\langle a_S\rangle^2}{\langle a_S^2\rangle - \langle a_S\rangle^2}, \tag{17a}$$

$$Z_{in} T = \frac{\langle a_{in}\rangle^2}{\langle a_{in}^2\rangle - \langle a_{in}\rangle^2}, \tag{17b}$$

$$Z_q T = \frac{\langle a_q\rangle^2}{\langle a_q^2\rangle - \langle a_q\rangle^2}. \tag{17c}$$

These figures of merit can be rather high when the variances of a_S, a_{in}, and a_q are small.

3. Cooling by thermal current effect

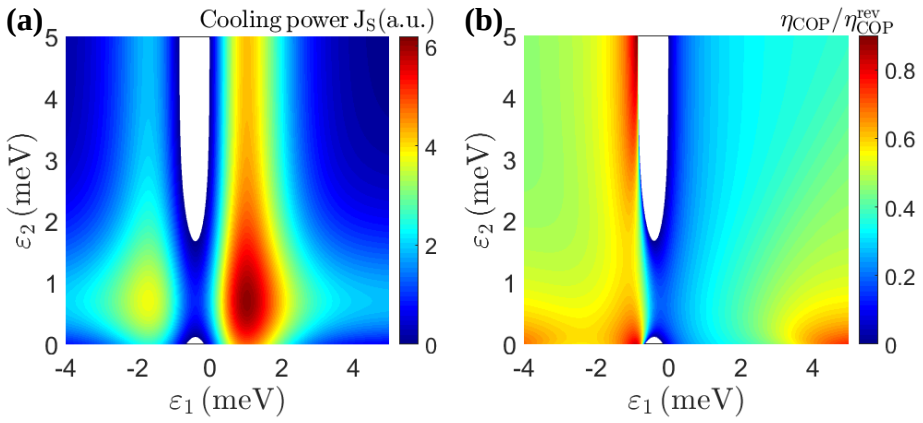

Figure S1: (a) Cooling power J_S and (b) COP ratio $\eta_{\rm COP}/\eta_{\rm COP}^{\rm rev}$ as functions of the QDs energies $E_{u1} = E_{d1} = \varepsilon_1$ and $E_{u2} = E_{d2} = \varepsilon_2$. Other parameters: $\mu_S = \mu_D = 0$, $k_BT_D = 1$ meV, $k_BT_H = 6$ meV, $k_BT_S = 0.6$ meV, $T_C = 1/(2/T_D - 1/T_H)$, $E_C = 1$ meV, and $\Gamma_0 = 0.1$ meV.

If we allow the energy configuration to be different between the pair of QDs $u1$ and $d1$ and the other pair of QDs $u2$ and $d2$ in a way that $E_{u1} = E_{d1} = \varepsilon_1$ and $E_{u2} = E_{d2} = \varepsilon_2$ with $E_C = 1$ meV, we can study how the cooling performance varies with the energies in the two channels, ε_1 and ε_2. From the Fig. S1(a), we find that the cooling power is maximized at $\varepsilon_1 \sim \varepsilon_2 \sim 1$ meV. As shown in Fig. S1(b), the COP ratio is rather optimized when $\varepsilon_1 \sim -1$ meV for large ε_2. This observation again demonstrates the efficiency-power trade off [5–7].

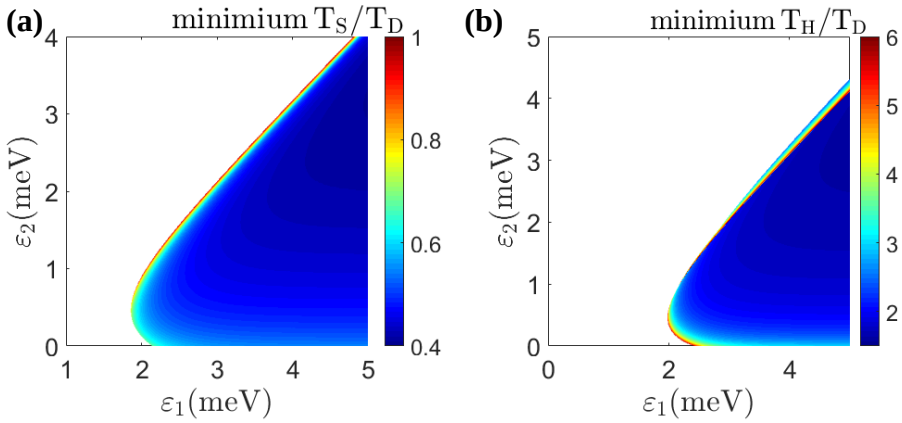

Figure S2: (a) The lowest temperature of source T_S that can be cooled down via the cooling by transverse current effect as functions of the QDs energies ε_1 and ε_2 for $k_BT_H = 6$ meV and $J_{in} = 0$. (b) The lowest temperature of the hot heat bath T H that can perform the cooling by transverse current effect as functions of the QDs energies ε_1 and ε_2 for $k_BT_S = 0.6$ meV and $J_{in} = 0$.

Finally we show that in our system it is indeed possible to realize the cooling by thermal current with vanishing total injected heat, $J_{in} = 0$, which termed as Maxwell's demon effect. Under the condition of

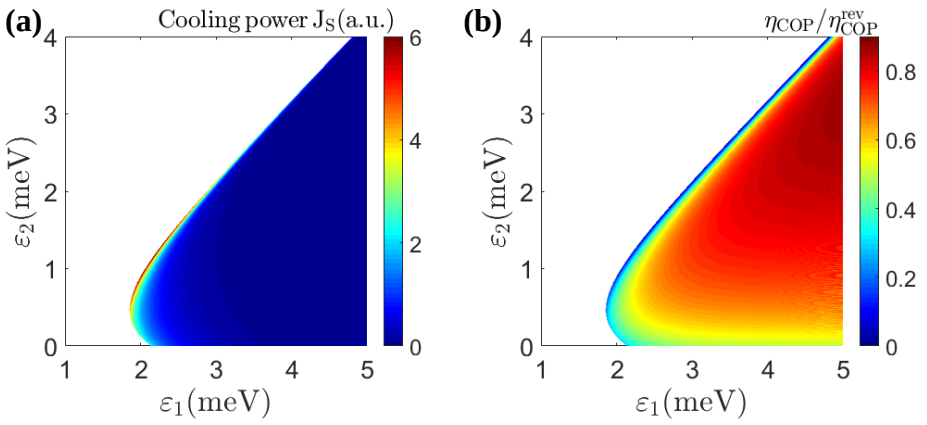

Figure S3: (a) Cooling power J_S and (b) COP ratio $\eta_{\rm COP}/\eta_{\rm COP}^{\rm rev}$ as functions of the QDs energies $E_{u1} = E_{d1} = \varepsilon_1$ and $E_{u2} = E_{d2} = \varepsilon_2$ for $J_{in} = 0$. Other parameters: $\mu_S = \mu_D = 0$, $k_B T_D = 1$ meV, $k_B T_H = 6$ meV, $T_C = 1/(2/T_D - 1/T_H)$, $E_C = 1$ meV, and $\Gamma_0 = 0.1$ meV.

Maxwell's demon, $J_{in} = 0$, we then begin to study the optimal energy configuration for the QD energies, $E_{u1} = E_{d1} = \varepsilon_1$ and $E_{u2} = E_{d2} = \varepsilon_2$ to obtain the lowest temperature of the source and the heat bath H. From Fig. S2(a), we find that the lowest temperature T_S when $\varepsilon_1 > \varepsilon_2$ and $\varepsilon_1 \geq 2$ meV. The white areas represent the parameter regions where the Maxwell's demon effect cannot be achieved, i.e., $J_S < 0$.

Similarly, we also study the minimum temperature of the heat bath H under the requirement of Maxwell's demon. In Fig. S2(b) we can see that it does not require too high temperature of the heat bath H in order to achieve the Maxwell's demon effect in the region $\varepsilon_1 > \varepsilon_2$. Meanwhile, we also find that the optimal parameter region for realization of Maxwell's demon effect is that $\varepsilon_1 > \varepsilon_2$ from Figs. S2(a) and S2(b).

In Fig. S3, we show the cooling power J_S and COP for the cooling by thermal current effect $\eta_{\rm COP}$ as functions of QD energies ε_1 and ε_2 for $J_{in} = 0$. In accordance with Fig. S2, the maximum of the cooling efficiency can be achieved when $\varepsilon_1 > \varepsilon_2$ but the value of the power is small. The results are consistent with the trade-off of power and efficiency [6–8].

References

[1] Sánchez R and Büttiker M 2011 *Phys. Rev. B* **83** 085428

[2] Jiang J H, Entin-Wohlman O and Imry Y 2012 *Phys. Rev. B* **85** 075412

[3] Jiang J H, Kulkarni M, Segal D and Imry Y 2015 *Phys. Rev. B* **92** 045309

[4] Zhang Y, and Lin G and Chen J 2012 *Phys. Rev. E* **91** 052118

[5] Entin-Wohlman O, Jiang J H, and Imry Y 2014 *Phys. Rev. E* **89** 012123

[6] Jiang J H 2014 *Phys. Rev. E* **90** 042126

[7] Lu J, Liu Y, Wang R, Wang C and Jiang J H 2019 *Phys. Rev. B* **100** 115438

[8] Proesmans K, Cleuren B and Van den Broeck C 2016 *Phys. Rev. Lett.* **116** 220601